 Related Commentary, page 13

Infiltration of CD4+ lymphocytes into the brain contributes to neurodegeneration in a mouse model of Parkinson disease

Vanessa Brochard,[1,2] Béhazine Combadière,[3] Annick Prigent,[1,2] Yasmina Laouar,[4] Aline Perrin,[1,2] Virginie Beray-Berthat,[1,2] Olivia Bonduelle,[3] Daniel Alvarez-Fischer,[1,2] Jacques Callebert,[5] Jean-Marie Launay,[5] Charles Duyckaerts,[1,2] Richard A. Flavell,[4,6] Etienne C. Hirsch,[1,2] and Stéphane Hunot[1,2]

[1]INSERM, UMR S679, Experimental Neurology and Therapeutics, Hôpital de la Salpêtrière, Paris, France. [2]Université Pierre et Marie Curie — Paris 06, UMR S679, Paris, France. [3]INSERM U543, Université Pierre et Marie Curie — Paris 06, Paris, France. [4]Department of Immunobiology, Yale University School of Medicine, New Haven, Connecticut, USA. [5]CR Claude Bernard, IFR6, Service de Biochimie, Hôpital Lariboisière, Assistance Publique — Hôpitaux de Paris, Paris, France. [6]Howard Hughes Medical Institute, Yale University School of Medicine, New Haven, Connecticut, USA.

Parkinson disease (PD) is a neurodegenerative disorder characterized by a loss of dopamine-containing neurons. Mounting evidence suggests that dopaminergic cell death is influenced by the innate immune system. However, the pathogenic role of the adaptive immune system in PD remains enigmatic. Here we showed that CD8+ and CD4+ T cells but not B cells had invaded the brain in both postmortem human PD specimens and in the 1-methyl-4-phenyl-1,2,3,6-tetrahydropyridine (MPTP) mouse model of PD during the course of neuronal degeneration. We further demonstrated that MPTP-induced dopaminergic cell death was markedly attenuated in the absence of mature T lymphocytes in 2 different immunodeficient mouse strains (*Rag1*$^{-/-}$ and *Tcrb*$^{-/-}$ mice). Importantly, similar attenuation of MPTP-induced dopaminergic cell death was seen in mice lacking CD4 as well as in *Rag1*$^{-/-}$ mice reconstituted with FasL-deficient splenocytes. However, mice lacking CD8 and *Rag1*$^{-/-}$ mice reconstituted with IFN-γ–deficient splenocytes were not protected. These data indicate that T cell–mediated dopaminergic toxicity is almost exclusively arbitrated by CD4+ T cells and requires the expression of FasL but not IFNγ. Further, our data may provide a rationale for targeting the adaptive arm of the immune system as a therapeutic strategy in PD.

Introduction

Parkinson disease (PD) is a neurodegenerative disorder characterized by the loss of dopamine-containing neurons (DNs) in the substantia nigra (SN) pars compacta (SNpc). Except for rare genetic forms, PD is a sporadic condition of unknown cause. Yet, several scenarios regarding the mechanisms by which DNs degenerate have been suggested, including mitochondrial dysfunction, oxidative stress, and the impairment of protein degradation machinery (1). In addition to these well-established pathomechanisms, there is mounting evidence from epidemiological, postmortem, and animal studies to suggest that innate neuroinflammatory processes associated with glial cell activation participate in the progression of DN cell death (2–6).

Far more enigmatic is the putative role of the adaptive immune system in PD pathogenesis. While several changes in cellular and humoral immune responses have been described in the peripheral immune system of PD patients, it remains unclear whether these alterations are primarily involved in the etiogenesis of PD or simply reflect secondary consequences of nigrostriatal pathway injury (5). Up to now, the hypothesis that the cellular arm of the adaptive immune system plays a role in neurodegeneration has been hampered by the fact that no clear demonstration of a prominent involvement of leukocytes at the site of neuronal injury has been provided in PD. Yet, the reports many years ago that cytotoxic T cells (Tc) can be found in massive numbers in the SN of a patient with PD (7) and that the density of IFN-γ–positive cells is markedly increased in brains of patients of with PD (8), suggest that T cell brain recruitment may be associated with nigrostriatal pathway injury in PD. In support of this view is the demonstration that the accumulation of T cells in the brain can be stimulated in mice by 1-methyl-4-phenyl-1,2,3,6-tetrahydropyridine–induced (MPTP-induced) DN injury (9). Yet, whether this immune response truly contributes to neurodegeneration and, if so, by what mechanisms remains to be established.

In this study, we sought to determine whether PD is associated with leukocyte brain infiltration within the affected SN region and, if so, whether this process contributes to DN degeneration. We found that both CD8+ and CD4+ T cells significantly invade the SN in postmortem specimens from patients with PD and in MPTP-intoxicated mice. We also show that removal of CD4+ but not of CD8+ T cells in mice greatly reduced MPTP-induced nigrostriatal DN cell death. Finally, we further demonstrate that the deleterious activity of infiltrated CD4+ T cells involved the Fas/FasL pathway but not Ifn-γ production.

Results

Lymphocyte brain infiltration in PD patients. To test the possibility that leukocytes infiltrate the brain parenchyma of PD patients, we performed immunohistochemical staining for various leuko-

Conflict of interest: The authors have declared that no conflict of interest exists.

Nonstandard abbreviations used: BBB, blood-brain barrier; DN, dopamine-containing neuron; GFAP, glial fibrillary acidic protein; gld, FasL-mutated generalized lymphoproliferative; MPP+, 1-methyl-4-phenylpyridinium; MPTP, 1-methyl-4-phenyl-1,2,3,6-tetrahydropyridine; PCNA, proliferating cell nuclear antigen; PD, Parkinson disease; *Rag1*, recombinase activating gene 1; SN, substantia nigra; SNpc, SN pars compacta; α-Syn, α-synuclein; Tc, cytotoxic T cell; *Tcrb*, T cell receptor β chain; TH, tyrosine hydroxylase.

Citation for this article: *J. Clin. Invest.* **119**:182–192 (2009). doi:10.1172/JCI36470.

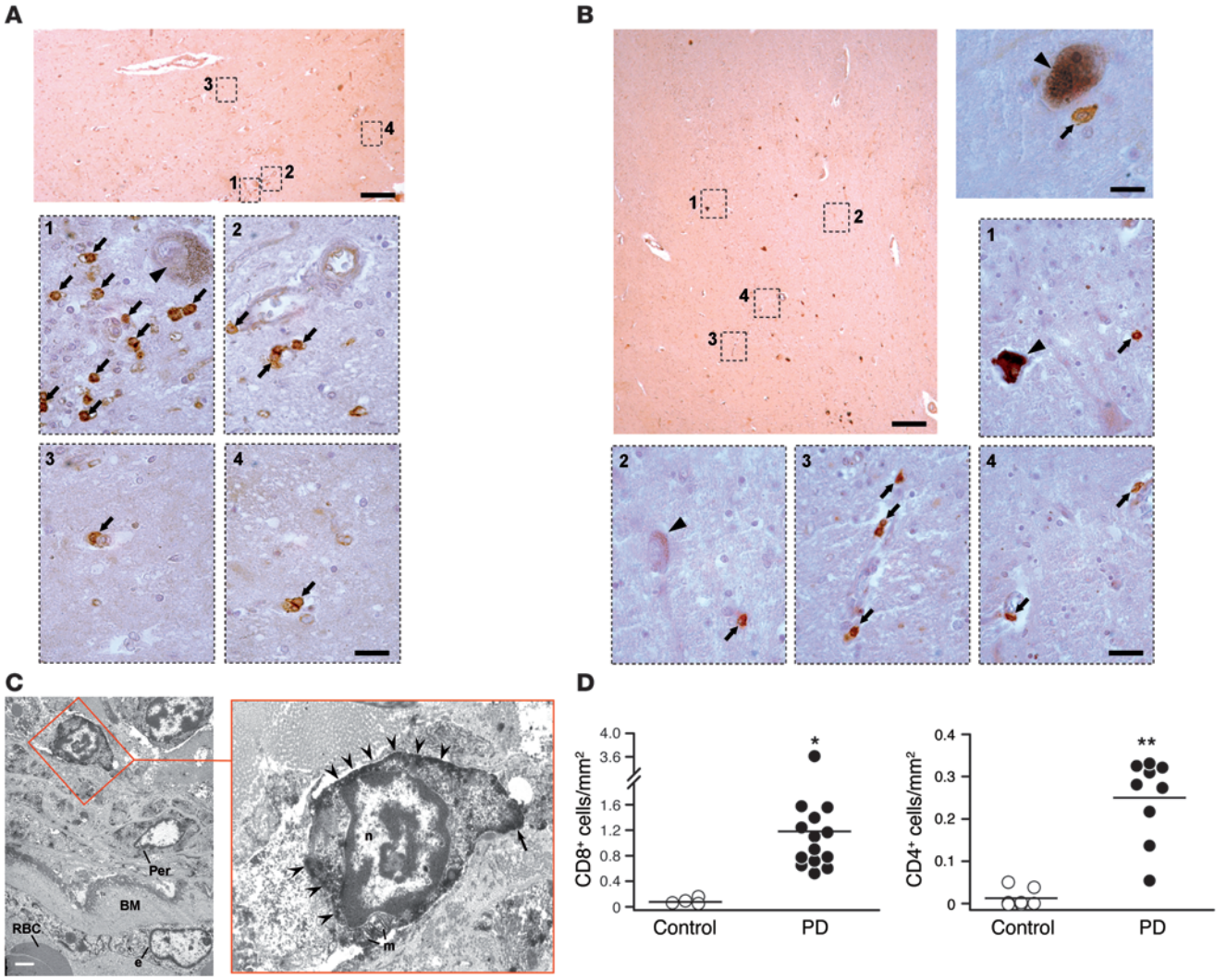

Figure 1

Lymphocyte infiltration in brains of patients of with PD. (**A**) CD8 and (**B**) CD4 immunostaining with hematein counterstain on mesencephalic transverse sections from PD patients. $CD8^+$ or $CD4^+$ T cells (arrows) are found in close contact with blood vessels or have migrated deep into the brain parenchyma close to neuromelanin-containing DNs (arrowheads). Note that brain staining for CD79α and CD20 (B cells) and CD57 (NK cells) was not detected in either group of patients. All antibodies were previously tested on human tonsil tissue sections taken as a positive control, and all of them gave the expected cellular staining (Supplemental Figure 1). Scale bars: 250 μm (upper panel in **A** and upper-left panel in **B**); 30 μm (dashed boxes); 15 μm (upper-right panel in **B**). (**C**) Ultrastructural view of an infiltrated $CD8^+$ T cell in the SNpc from a parkinsonian patient. Parenchymal $CD8^+$ T cells display a small cytoplasmic volume, membrane-type CD8 staining (arrowheads), and a uropod-like cytoplasmic extension, usually involved in T cell motility (arrow). Per, pericyte; BM, basal membrane; e, endothelial cell; m, mitochondria; n, nucleus. Scale bar: 4 μm. (**D**) Density of infiltrated $CD8^+$ (left panel) and $CD4^+$ T cells (right panel) in the SNpc of parkinsonian patients (n = 14 and 9 for CD8 and CD4 staining, respectively) and age-matched control subjects (n = 4 and 7 for CD8 and CD4 staining, respectively). Bars represent the mean density. $^*P < 0.05$, $^{**}P < 0.001$ compared with controls (Student's t test).

cyte-specific markers (10) on postmortem human brain (for antibody description, see Supplemental Table 1; supplemental material available online with this article; doi:10.1172/JCI36470DS1). Positive staining was observed for CD8 and CD4 but not for B cell and NK cell markers. Within the SNpc, $CD8^+$ and $CD4^+$ T cells were found either in close contact with blood vessels or in the vicinity of melanized DNs (Figure 1, A and B). These cells displayed a typical lymphocyte morphology that was further confirmed by electron microscopy analysis. At the ultrastructural level, parenchymal $CD8^+$ T cells displayed small cytoplasmic volume, membrane-type CD8 staining, and, in some cases, uropod-like cytoplasmic extension, usually involved in T cell motility (Figure 1C). Importantly, quantitative analysis revealed a significant increase (10-fold in average) in the density of $CD8^+$ and $CD4^+$ T cells in the SNpc but not in the nonlesioned red nucleus from PD patients compared with age-matched control subjects (Figure 1D and Supplemental Table 2).

MPTP-induced DN lesion stimulates extravasation of lymphocytes into the brain. The above data suggest that migration of peripheral lymphocytes within the CNS is associated with nigrostriatal pathway injury in PD. Yet, although postmortem studies in humans are essential to establish that immune cell infiltration is characteristic

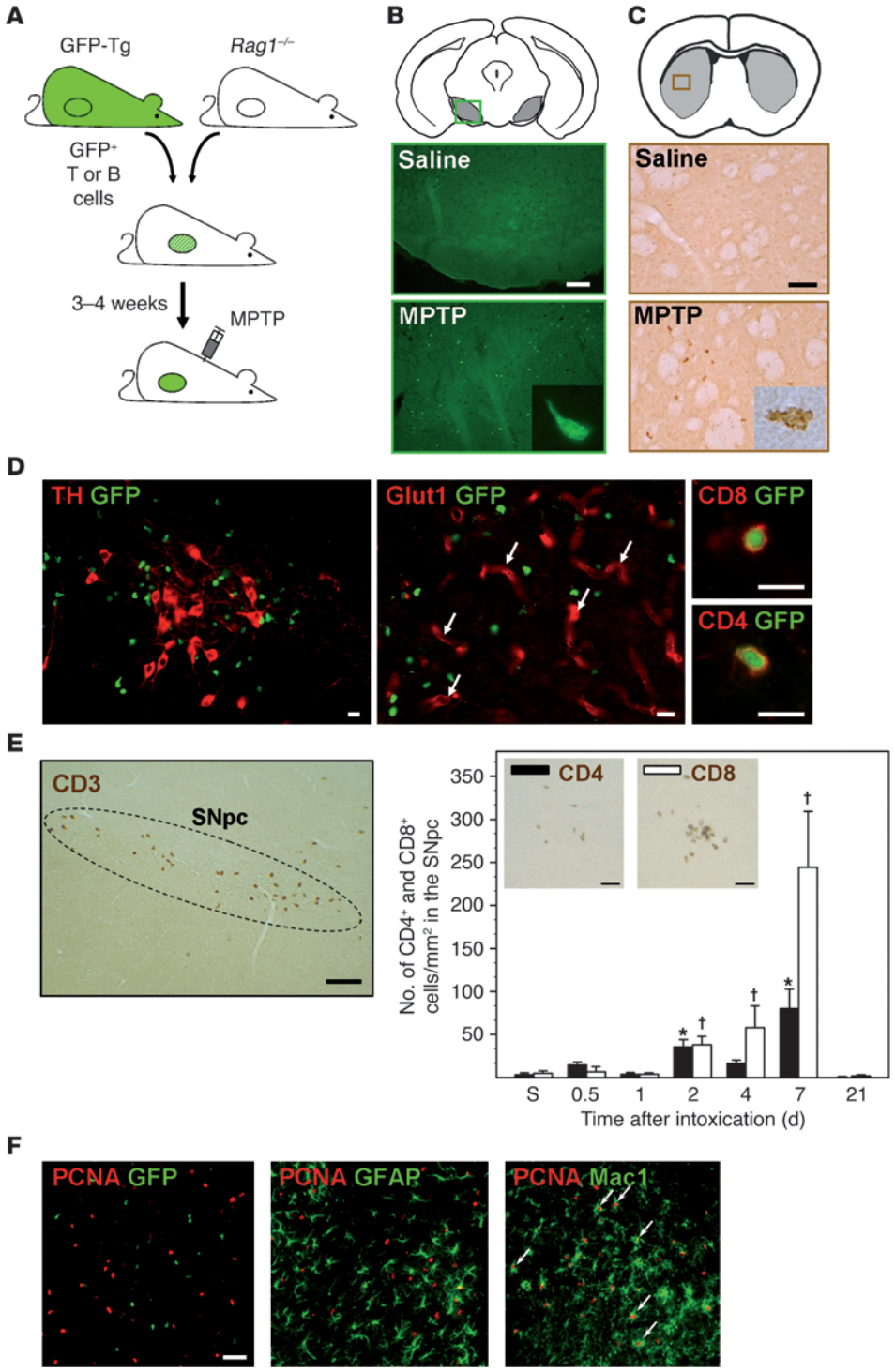

Figure 2
MPTP-induced nigrostriatal pathway injury stimulates T cell brain infiltration in mouse. (**A**) Schematic representation of the experimental approach (see Methods). The green circle within reconstituted mice refers to the lymphoid compartments replenished with GFP+ cells. (**B**) GFP+ T cell infiltration in the SNpc and (**C**) striatum following MPTP intoxication. Numerous GFP+ T cells can be seen in the SNpc 2 days after MPTP but not saline exposure. GFP+ T cells are also found in the striatum from intoxicated mice, though there are far fewer than in the SNpc. Scale bars: 300 μm (**B**); 100 μm (**C**); 10 μm (insets). (**D**) Immunofluorescent staining for TH, Glut1, CD8, or CD4. Note that infiltrated GFP+ T cells are clustered within the SNpc in close proximity to TH+ DNs. Transmigrated GFP+ T cells are not found in the lumen of Glut1+ blood vessels (arrows) and consist of both CD8+ and CD4+ T cell subsets. Scale bars: 20 μm. (**E**) T cell brain infiltration in MPTP-treated C57BL/6 inbred mice. CD3 immunostaining showing numerous T lymphocytes within the SNpc (dashed line) from MPTP-treated mice (left panel). Scale bar: 100 μm. Kinetic of nigral CD4+ and CD8+ T cell (insets) density after MPTP exposure (right panel). S, saline. Data points represent the mean ± SEM. $^{*}P < 0.01$ compared with saline- and MPTP-treated mice at day 4 after MPTP exposure; $^{\dagger}P < 0.01$ compared with saline-treated controls (Tukey post-hoc analysis). Scale bars: 50 μm. (**F**) Double immunofluorescence staining for PCNA and GFP and GFAP or Mac1. Note that PCNA+ cells in the SNpc never colocalize with GFP+ or GFAP+ cells, whereas they superpose perfectly with Mac-1+ macrophages/microglial cells (arrows). Scale bar: 50 μm.

of the disease, they cannot provide information about the dynamic and functional relevance of such mechanisms. To address this issue, we conducted in vivo experiments using the well-characterized MPTP-intoxicated mouse model of PD (1). Although it is not a phenocopy of human disease, this noninvasive model provides a unique means to study non-cell autonomous pathomechanisms, as it recapitulates many of the hallmarks of PD, including DN loss, attenuation of striatal dopamine, and glial cell–associated inflammatory processes. To easily track the migration of peripheral leukocytes independently of their phenotypic traits, we first used a passive transfer strategy that consisted of transferring GFP-tagged T or B cells into recombinase activating gene 1–deficient (*Rag1*-deficient) mice, which lack mature lymphocytes. Recipient animals with reconstituted lymphoid organs were then treated with MPTP or saline solution (Figure 2A and Supplemental Figure 2). Unlike GFP+ B cells (data not shown), we found GFP+ T cells in the SNpc

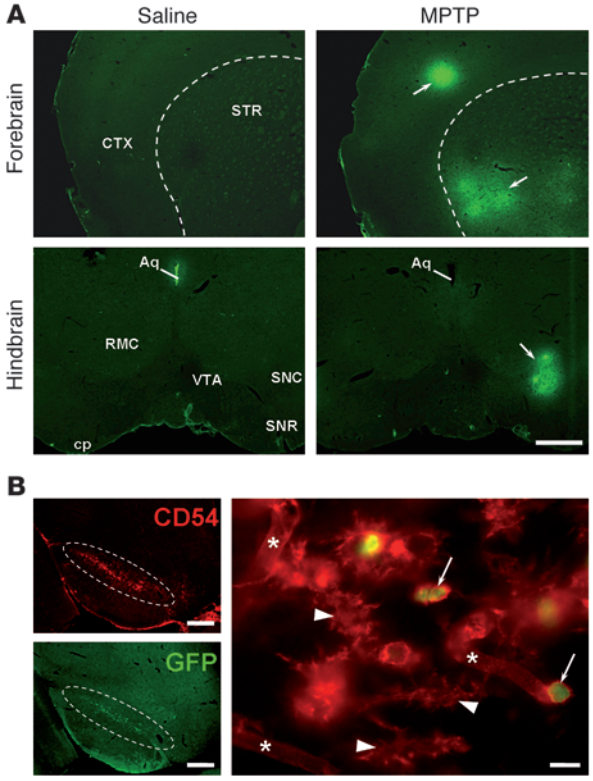

Figure 3
Mechanism of lymphocyte entry into the brain. (**A**) Immunofluorescent staining for serum albumin on brain sections (forebrain and hindbrain levels are shown) from mice sacrificed 6 hours after the last MPTP or saline injection. Patches of staining (arrows) are detected in various brain areas at 6 hours following MPTP exposure but not after saline treatment. The dashed line indicates the boundary between the striatal and cortical areas. CTX, cortex; STR, striatum; RMC, magnocellular part of the red nucleus; VTA, ventral tegmental area; SNC, substantia nigra compacta; SNR, substantia nigra reticulata; Aq, aqueduct of Sylvius; cp, cerebral peduncle. Scale bar: 300 μm. (**B**) Immunostaining for CD54/ICAM-1 (red) on mesencephalic sections from MPTP-intoxicated GFP$^+$ T cell–reconstituted *Rag*$^{-/-}$ mice. The expression pattern of CD54 overlaps with that of the GFP$^+$ T cell infiltrate within the SNpc (dashed line) (left panel). At higher magnification (right panel), CD54 expression is visible on GFP$^+$ T cells (arrows), blood vessels (asterisks), and branched glial cells (arrowheads). Scale bars: 300 μm (left panel); 10 μm (right panel).

and striatum after MPTP treatment (Figure 2, B and C). Most, if not all, other brain structures but DN-containing regions were devoid of T cell infiltrate, indicating the region-specific extravasation of these immune cells (Supplemental Figure 3). Brain sections immunostained for tyrosine hydroxylase (TH) show GFP$^+$ T cells within the SNpc clustered in close proximity to TH-expressing DNs (Figure 2D). Furthermore, infiltrated T cells had clearly transmigrated through the brain parenchyma, since most of them were found to be excluded from the lumen of blood vessels identified by Glut1 immunostaining (Figure 2D). Finally, both CD8$^+$ and CD4$^+$ T cell subtypes were found to be recruited (Figure 2D).

To ensure that the infiltration of T cells into the brain observed in our graft-based experimental model was not merely an artifact related to the methodology, we looked at leukocyte transmigration in MPTP-intoxicated C57BL/6J inbred mice, using immunohistochemistry for the T cell–specific marker CD3. In these conditions, a similar T cell infiltration process was observed (Figure 2E). When compared with the time course of glial cell activation, CD3$^+$ T cell brain infiltration was found to arise after the increase of CD11b$^+$ microglial cells (i.e., 12 hours post-MPTP intoxication) but concomitantly with astrogliosis (Supplemental Figure 4). Consistent with our postmortem findings, nigral CD8$^+$ T cells were more abundant than CD4$^+$ T cells, and transmigration occurred at day 2 after treatment, increased continuously for up to 7 days, and had totally ceased at 21 days (Figure 2E). Such dynamics are therefore compatible with a possible role of activated microglial cells in the brain region–specific recruitment of T cells.

The continuous nigral accumulation of T cells indicates that lymphocytes could clonally expand into the brain parenchyma. To test such a possibility, we surveyed the expression of proliferating cell nuclear antigen (PCNA), taken as a marker of dividing cells, at 0.5, 1, 2, 4, and 7 days after the last MPTP injection. As shown in Figure 2F, while we observed numerous PCNA$^+$ cells in the SNpc after MPTP intoxication, none of them were found to colocalize with either GFP$^+$ T cells or glial fibrillary acidic protein–positive (GFAP-positive) astrocytes at all the time points analyzed. Instead, most of these cells also expressed the myeloid marker CD11b, suggesting that infiltrated macrophages and/or resident microglial cells multiply at the site of injury. Thus, accumulation of T cells may indicate a continuous extravasation process, at least up to 7 days after neurotoxin exposure. Yet, the number of CD3$^+$ T cells within the SNpc was found to dramatically decrease shortly after this accumulation (i.e., at day 9) (Supplemental Figure 5A), raising the possibility that they could be rapidly eliminated by apoptotic cell death due to regulatory mechanisms aimed at terminating the immune response. To test this, we looked for morphological criteria as well as molecular changes indicative of apoptosis in the entire SNpc and ventral tegmental area of animals sacrificed 7 and 9 days after systemic MPTP administration. Immunohistochemistry for CD3 coupled with thionin counterstaining revealed the presence of apoptotic cells characterized by shrinkage of cellular body, chromatin condensation, and presence of distinct, round, well-defined chromatin clumps (Supplemental Figure 5B). Whereas apoptotic cells were found in all MPTP-treated mice analyzed at day 7 and 9 (n = 10 and 5, respectively), they were not observed in saline-injected controls. In few instances, these cells have retained some CD3 staining, attesting their T cell origin (Supplemental Figure 5C). Additional evidence for T cell apoptosis was obtained from double immunofluorescence staining for CD3 and activated caspase-3. Thus, some CD3$^+$ T cells were found to be positive for the p17 fragment of activated caspase-3 (Supplemental Figure 5D).

Since a previous report indicated that the blood-brain barrier (BBB) may be dysfunctional in PD patients (11), we examined whether MPTP-associated BBB disruption could account for a passive entry of lymphocytes into the brain. A time course of BBB leakage from 6 hours to 7 days after MPTP administration was determined by assessing serum albumin and immunoglobulin extravasation. Our data reveal that MPTP induces a widespread and transitory serum protein leakage (detectable at 6 hours but absent from 12 hours after MPTP treatment), contrasting therefore with the cell type– and region-specific leukocyte extravasation process (Figure 3A). To further explore the mechanism of T cell extravasation, we surveyed the expression of ICAM-1/CD54,

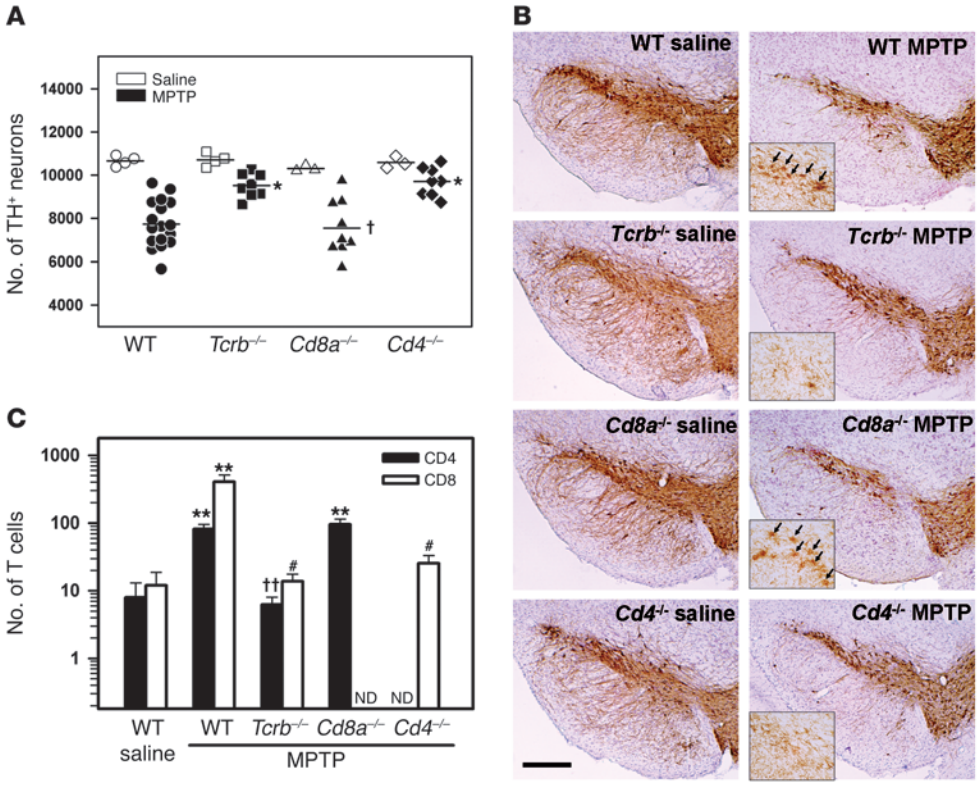

Figure 4

Mice deficient in CD4+ T cells are more resistant to MPTP. (**A**) Quantification of TH+ DNs in the SNpc at day 7 after MPTP (4 × 18 mg/kg) or saline treatment in WT, *Tcrb*$^{-/-}$, *Cd8a*$^{-/-}$, and *Cd4*$^{-/-}$ mice. Bars represent the mean number of total nigral TH+ DNs. Open symbols indicate saline-treated animals and filled symbols indicate MPTP-treated animals. Each symbol represents 1 individual animal. A significant protection against MPTP-induced DN cell loss is observed in *Tcrb*$^{-/-}$ and *Cd4*$^{-/-}$ mice but not in *Cd8a*$^{-/-}$ animals as compared with their WT littermates. $^{*}P < 0.05$ compared with MPTP-treated WT and *Cd8a*$^{-/-}$ mice; $^{\dagger}P = 0.956$ compared with MPTP-treated WT littermates (Tukey post-hoc analysis). Nissl+ cell counts confirmed that TH+ cell loss was not a consequence of downregulated expression of TH (data not shown). (**B**) Representative photomicrographs of mesencephalic sections immunostained for TH with Nissl counterstain from saline- or MPTP-treated WT and lymphocytic deficient mice. Insets show Mac-1+ microglial cells (arrows) in the SNpc from the same animals. Scale bar: 300 μm; 100 μm (insets). (**C**) Quantification of the total number of infiltrated CD4+ and CD8+ T cells in the SNpc from MPTP-treated WT and lymphocytic deficient mice. MPTP-treated *Cd8a*$^{-/-}$ mice display as many CD4+ T cells as MPTP-treated WT littermates. $^{**}P < 0.05$ compared with saline-injected WT mice (Mann-Whitney *U* test). $^{\dagger\dagger}P < 0.001$ compared with MPTP-treated WT and *Cd8a*$^{-/-}$ mice; $^{\#}P < 0.001$ compared with MPTP-treated WT mice (Dunn test). ND, not detected.

an immunoglobulin-like cell adhesion molecule, involved in leukocyte adherence and transendothelial migration at sites of inflammation (12). Whereas CD54 was barely detectable in controls (data not shown), we observed a marked increase in CD54 immunostaining within the SNpc at the site of T cell infiltration following MPTP intoxication (Figure 3B). Blood vessels, glial cells, and T cells were all intensely positive, indicating possible cross-interactions among these cellular actors.

Mice deficient in cell-mediated immunity are more resistant to MPTP. Investigations dedicated to unraveling the role of infiltrated T cells in various models of neuronal injury have led to opposite conclusions (13, 14). To determine whether T cell accumulation in the SNpc following MPTP intoxication is beneficial or harmful to DNs, we compared the effects of the toxin in T cell receptor β chain mutant mice lacking mature T lymphocytes (*Tcrb*$^{-/-}$) (15) and in their WT littermates. We found that whereas only 72% of the nigral TH+ DNs survived MPTP injection in WT mice, 91% of these neurons survived in *Tcrb*$^{-/-}$ mice treated with a similar MPTP regimen (Figure 4, A and B). Importantly, the decrease in MPTP-induced DN loss in *Tcrb*$^{-/-}$ mice correlated with a reduction in the number of infiltrated T cells to a level similar to that of saline-injected animals (Figure 4C). Residual T cell infiltration in *Tcrb*$^{-/-}$ mice may come from the small number (about 8% of the WT level) of cells remaining in the thymus of these mutants (15).

Given the apparent harmful behavior of infiltrated T cells, we next investigated whether CD8+ and/or CD4+ T cells could mediate such a detrimental function. To that end, we intoxicated mice homozygous for either a targeted mutation of *Cd8a* or *Cd4*, characterized by a deficiency in functional Tc and Th, respectively (16, 17). Whereas MPTP induced a comparable level of DN cell death in *Cd8a*$^{-/-}$ mice as in WT littermates, we observed a marked reduction in TH+ cell loss in *Cd4*$^{-/-}$ mice (Figure 4, A and B). Interestingly, the rate of DN survival in *Cd4*$^{-/-}$ mice was comparable to that of *Tcrb*$^{-/-}$ animals, suggesting that most of the deleterious outcome associated with infiltrated T cells is mediated by the CD4+ Th subset. In support of this idea, susceptible WT and *Cd8a*$^{-/-}$ mice exhibited a similar number of infiltrated CD4+ T cells following MPTP exposure (Figure 4C). However, there were no significant differences in the extent of loss in striatal levels of dopamine, 3-4-dihydroxyphenylacetic acid (DOPAC), and homovanillic acid (HVA) between

Table 1
Striatal monoamine levels (pM/mg tissue)

	Dopamine	DOPAC	HVA
Saline			
WT ($n = 5$)	82.3 ± 7.5	15.4 ± 1.9	10.1 ± 1.0
Tcrb$^{-/-}$ ($n = 3$)	85.4 ± 12.7	15.8 ± 3.0	9.5 ± 1.6
Cd8a$^{-/-}$ ($n = 3$)	84.6 ± 4.1	16.0 ± 1.0	9.9 ± 0.9
Cd4$^{-/-}$ ($n = 3$)	65.0 ± 8.9	15.7 ± 2.3	8.7 ± 1.4
MPTP			
WT ($n = 5$)	1.7 ± 0.3	1.8 ± 0.2	3.2 ± 0.4
Tcrb$^{-/-}$ ($n = 4$)	2.8 ± 0.4	2.5 ± 0.3	3.7 ± 0.5
Cd8a$^{-/-}$ ($n = 4$)	4.9 ± 1.6	2.2 ± 0.3	3.2 ± 0.1
Cd4$^{-/-}$ ($n = 4$)	3.5 ± 0.5	3.0 ± 0.5	4.5 ± 0.6

Striatal dopamine, DOPAC, and HVA levels in WT, *Tcrb*$^{-/-}$, *Cd8a*$^{-/-}$, and *Cd4*$^{-/-}$ mice at 7 days after the last MPTP injection do not differ ($P > 0.05$; Kruskal-Wallis test) between groups. Data represent mean ± SEM for the indicated number of mice. DOPAC, 3-4-dihydroxyphenylacetic acid; HVA, homovanillic acid.

mutant mice and their WT littermates after the administration of MPTP, implying that striatal T cell infiltration is not a major component of dopaminergic fibber injury (Table 1). Importantly, reduced MPTP metabolism in mutant mice is not likely to account for the observed neuroprotection, as striatal 1-methyl-4-phenylpyridinium (MPP^+) content after a single systemic MPTP injection did not differ between genotypes (Table 2). Moreover, consistent with the partial resistance of *Tcrb*$^{-/-}$ and *Cd4*$^{-/-}$ mice to MPTP, midterm (2–7 days) microglial cell activation was almost completely abolished in mutant mice (Figure 4B).

The Fas/FasL pathway is required for CD4 T cell–dependent DN toxicity. The finding that CD4-deficient mice are partially protected against MPTP-induced injury suggests that Th-mediated deleterious mechanisms are engaged and instrumental in DN demise. Cytokines, including IFN-γ, and membrane bound ligands, such as FasL, represent 2 major classes of molecules mediating effector functions of CD4 Th (e.g., macrophage activation). Interestingly, it has been shown that IFN-γ was a contributing factor in the death of DNs by regulating microglial activity (18). In fact, we found that IFN-γ expression was upregulated in the ventral midbrain 2 days after MPTP exposure, which coincided with the first wave of $CD4^+$ T cell brain infiltration (Supplemental Figure 6A). To analyze the putative deleterious role of lymphocyte-derived IFN-γ, we passively transferred total splenocytes isolated from either WT or IFN-γ–deficient mice into recipient *Rag1*$^{-/-}$ animals. Consistent with the deleterious role of T cells as previously evidenced in *Tcrb*$^{-/-}$ mice, we noticed that MPTP-induced injury in immunodeficient *Rag1*$^{-/-}$ mice was significantly less severe than in WT littermates (Figure 5, A and B). Importantly, this partial resistance was completely reversed when spleen cells from either WT or *Ifng*$^{-/-}$ mice were passively transferred prior to MPTP intoxication (Figure 5A). Thus, lymphocyte-derived IFN-γ is not likely to be required for T cell–mediated DN cell death. In support for this assertion, *Ifng*$^{-/-}$ mice and their WT littermates were found to be equally sensitive to MPTP-induced DN cell death using an identical intoxication paradigm (Supplemental Figure 6B). Therefore, we next considered the involvement of a Fas-based mechanism. To test this, we took advantage of the FasL-mutated generalized lymphoproliferative (*gld*) mice that bear a point mutation in the extracellular domain of FasL (CD95L), resulting in a dramatic decrease of affinity to its receptor Fas (19). Thus, we compared the MPTP susceptibility of *Rag1*$^{-/-}$ recipients that received spleen cells from either *gld* or C57BL/6J donors (designated *gld* rec. *Rag1*$^{-/-}$ and WT rec. *Rag1*$^{-/-}$, respectively). In WT rec. *Rag1*$^{-/-}$ mice, MPTP caused as much DN loss as in WT animals (Figure 5, A–C). In sharp contrast, both nonreconstituted *Rag1*$^{-/-}$ and *gld* rec. *Rag1*$^{-/-}$ mice exposed to a similar dose of MPTP exhibited a significantly smaller reduction in the number of nigral DNs (Figure 5, B and C). The protection gained in *gld* rec. *Rag1*$^{-/-}$ mice was consistently within a similar range to that observed in *Cd4*$^{-/-}$ animals (Figure 4A and Figure 5B). Furthermore, this protective effect was not likely due to altered extravasation potency of gld-derived splenocytes, as a similar number of brain infiltrated $CD4^+$ T cells were observed between MPTP-treated WT rec. *Rag1*$^{-/-}$ and *gld* rec. *Rag1*$^{-/-}$ animals (mean number of $CD4^+$ T cells in the SNpc ± SEM, 81.6 ± 22.5 and 95.5 ± 38.2, respectively; $P = 0.55$, Mann-Whitney U test). Together, these results suggest that $CD4^+$ Th-mediated DN cell death requires the expression of a functional FasL but not IFN-γ.

Discussion

Mounting evidence supports the notion that innate immunity significantly contributes to dopaminergic neurodegeneration in PD (1). By contrast, although altered cellular and humoral functions have been reported in the peripheral immune system of PD patients, the role of adaptive immunity in the pathogenesis of this disorder has remained much more elusive (5, 20). Among these peripheral immune changes, the significant increased ratio of $CD8^+$ Tc to $CD4^+$ Th and of IFN-γ–producing to IL-4–producing T cells suggests the existence of a disease-associated shift to a Tc1/Th1-type immune response, which may reflect and/or contribute to the harmful brain inflammatory reaction (21). Nonetheless, a role for the cellular arm of the adaptive immune system in neurodegeneration is curbed by the fact that no clear demonstration of a prominent involvement of leukocytes at the site of neuronal injury has been provided in PD. In this study, we present evidence that peripheral T cells migrate to and accumulate in the brain parenchyma during parkinsonism. Importantly, we have shown that $CD4^+$ but not $CD8^+$ T cells are deleterious to DNs, which suggests that the adaptive immune system may contribute to disease progression in PD.

It is now well established that the CNS is not only continuously monitored by T cells (22) but also massively invaded by peripheral leukocytes in neuropathological circumstances (23). In agreement with the seminal but rather preliminary observation by McGeer and colleagues, showing a substantial presence of $CD8^+$ T cells in the brain from one PD case (7), we now provide strong quantitative evidence from a large number of individuals that both $CD8^+$ and $CD4^+$ T lymphocytes markedly accumulate in the SNpc

Table 2
Striatal MPP^+ content after MPTP injection

Genotypes	MPP^+ (ng/mg tissue)
WT	7.09 ± 2.95
Tcrb$^{-/-}$	6.00 ± 2.55
Cd8a$^{-/-}$	7.89 ± 2.17
Cd4$^{-/-}$	5.29 ± 2.16

Striatal MPP^+ levels in WT, *Tcrb*$^{-/-}$, *Cd8a*$^{-/-}$, and *Cd4*$^{-/-}$ mice at 90 minutes after a single MPTP injection do not differ ($P = 0.87$; Kruskal-Wallis test) between groups. Data represent mean ± SEM for 5 mice per group.

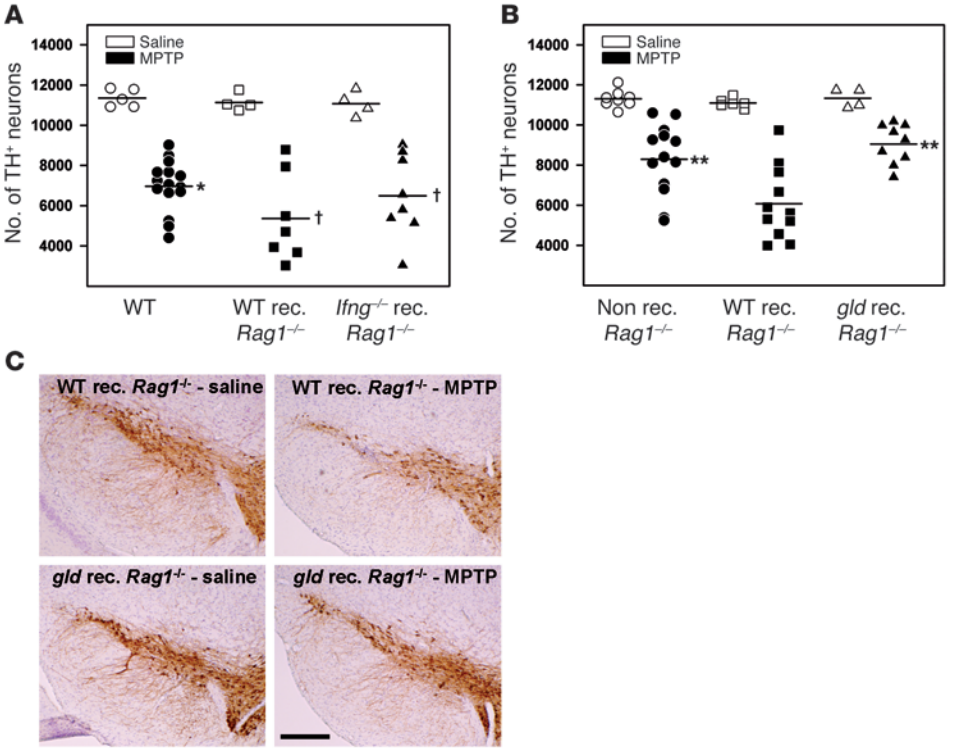

Figure 5

FasL, but not IFN-γ, is required for T cell–mediated DN toxicity in MPTP mouse. (**A**) Quantification of TH+ DNs in the SNpc at day 7 after MPTP (4 × 18 mg/kg) or saline treatment in WT and *Rag1*$^{-/-}$ mice reconstituted with spleen cells from either C57BL/6 inbred or *Ifng*$^{-/-}$ donors. All groups of animals are equally sensitive to MPTP-induced DN injury. *$P < 0.05$ compared with their saline counterparts; †$P < 0.05$ compared with their saline counterparts but not different from MPTP-treated WT mice (Tukey post-hoc analysis). (**B**) Quantification of TH+ DNs in the SNpc at day 7 after MPTP (4 × 18 mg/kg) or saline treatment in nonreconstituted *Rag1*$^{-/-}$ mice (non rec. *Rag1*$^{-/-}$) and in *Rag1*$^{-/-}$ mice reconstituted with spleen cells from either C57BL/6 or *gld* donors (WT rec. *Rag1*$^{-/-}$ and *gld* rec. *Rag1*$^{-/-}$, respectively). Nonreconstituted *Rag1*$^{-/-}$ mice and *gld* rec. *Rag1*$^{-/-}$ mice are partially protected against MPTP-induced DN loss as compared with WT rec. *Rag1*$^{-/-}$ animals. **$P < 0.01$ compared with MPTP-intoxicated WT rec. *Rag1*$^{-/-}$ mice (Tukey post-hoc analysis). (**A** and **B**) Open symbols indicate saline-treated animals and filled symbols indicate MPTP-treated animals. Each symbol represents 1 individual animal. Bars represent the mean number of total nigral TH+ DNs. (**C**) Representative photomicrographs of mesencephalic sections immunostained for TH with Nissl counterstain from saline- or MPTP-treated WT rec. *Rag1*$^{-/-}$ and *gld* rec. *Rag1*$^{-/-}$ mice. Scale bar: 300 μm.

of PD patients. Consistent with a previous report (9), we found that experimental lesion of the nigrostriatal pathway in MPTP-intoxicated mice results in a similar brain accumulation of T cells. Yet, brain accumulation of T cells following MPTP intoxication was not restricted to the SNpc. Indeed, other catecholaminergic areas known to be moderately injured following MPTP treatment (24) were also invaded, albeit to a lower extent. This extravasation of lymphocytes is not likely to be a generalized nonspecific leukocyte response, as (a) other leukocyte subsets, including B cells and NK cells, were not detected in the lesioned SNpc, and (b) an increased occurrence of T cells was not observed in nonlesioned brain areas, suggesting that this process does not simply reflect an overall enhancement of lymphocyte patrolling. Altogether, these findings indicate that, as with the glial cell reaction previously described, T cell brain infiltration in PD most certainly represents a secondary and highly regulated pathogenic event associated with neuronal cell death. Such a cellular and site-specific brain immune response is not likely to be caused by a massive disruption of the BBB, for which little evidence exists in PD (25, 26) and which remains controversial in MPTP-intoxicated mice (27, 28). We showed a widespread BBB leakage that occurred shortly (6 hours) after neurotoxin exposure and was rapidly resolved (by 12 hours after MPTP treatment), well before lymphocytic invasion. Taken together, these findings argue that lymphocyte brain infiltration is not a passive phenomenon. Instead, molecular and cellular changes associated with neuronal injury are likely to regulate this site-specific brain recruitment of T cells. Possible mechanisms may involve early microglial cell activation and innate neuroinflammatory processes that could modify the local microenvironment. In line with this, we found an upregulated expression of the ICAM-1 adhesion molecule on both capillaries and glial cells, which may participate in the attachment of leukocytes to the vascular endothelium and their diapedesis (29). Interestingly, a similar ICAM-1 overexpression was recently described in both the SN of patients with PD and MPTP-intoxicated monkeys (30). Although the level of T cell brain accumulation was found to be higher in the disease model than in PD patients, one has to consider that the human disease progresses over several decades, whereas it only lasts 1 to 2 weeks in mouse model. Moreover, investigations performed on human postmortem tissue most often address late pathomechanisms and can not therefore predict the intensity of the lymphocyte infiltration process, which might be greater during earlier stages of the disease. Given that incidental Lewy body disease is considered by some authors to be a presymptomatic form of PD (31), it might be valuable to explore such lymphocytic invasion in those patients. Finally, it is worth noting that the distribution of T cell accumulation within the SNpc from PD patients is much more heterogeneous than that in MPTP mice. Indeed, in few instances, as shown in Figure 1, infiltrating T cells in brains of patients of with PD were found to be clustered around the few remaining pigmented DNs, whereas they were virtually absent in advanced depigmented areas. Such distribution suggests that the number of T cells reaching the target neurons is conceivably substantial and strengthens their possible involvement in DN cell demise.

A major contribution of our study is the demonstration that infiltration of T cells into the brain actively participates in DN degeneration. A decreased vulnerability of DNs to MPTP toxicity

associated with the removal of mature T lymphocytes was achieved by 2 different genetic immune defects (*Rag1*$^{-/-}$ and *Tcrb*$^{-/-}$), thus supporting a role for the cellular arm of the adaptive immune system in experimental parkinsonism. Our results are in agreement with a recent study, showing a similar neuropathological improvement in MPTP-intoxicated SCID mice (32). Notably, our data further reveal that different T cell subsets do not contribute equally to DN cell death. Indeed, while the predominance of infiltrated CD8$^+$ over CD4$^+$ T cells was consistently observed both in PD patients and MPTP-intoxicated mice, removal of the CD8$^+$ T cell subset in *Cd8a*$^{-/-}$ mice did not mitigate MPTP injury. In sharp contrast, the Th deficiency achieved in *Cd4*$^{-/-}$ mice conferred as much neuroprotection as in *Rag1*$^{-/-}$ and *Tcrb*$^{-/-}$ animals, suggesting that CD4$^+$ T cells mediate most if not all the deleterious activity associated with the adaptive immune response.

Since infiltrated T cells highly express ICAM-1 as well as lymphocyte function-associated antigen-1 (LFA-1) and CD44 (9, 30), we believe that most of them could be recruited from an activated/memory population. A mechanism of peripheral leukocyte activation secondary to MPTP intoxication has recently been proposed (32). In this model, nitrotyrosine modification within α-synuclein (α-Syn) promotes an antigen-specific T cell response in draining lymph nodes. After migrating into the injured brain areas, these antigen-specific T cells could undergo further activation and promote microglial cell–dependent neurodegeneration through cytokine release. Although the differential contribution of CD8$^+$ versus CD4$^+$ T cells in this deleterious immune response was not addressed by the authors, their prediction analysis of α-Syn–specific T cell epitopes suggested a significant potential for CD4$^+$ T cells of mice expressing IA^k or IA^b MHC class II molecules to respond to nitrated epitopes of α-Syn. These data, taken in conjunction with our present findings, support a model in which MPTP-induced brain antigen modification most likely generates a secondary and harmful Th response contributing to DN degeneration.

Looking at the cytotoxic mechanism mediated by the CD4$^+$ T cell response following nigrostriatal pathway injury, we found that T cell expression of FasL but not IFN-γ was required. It has been shown that IFN-γ is critical in microglial-mediated loss of DNs in MPTP-intoxicated mice (18). Yet, using 2 different experimental approaches, i.e., total and cell-specific IFN-γ deletion, we were unable to show a major role for this proinflammatory cytokine in DN cell demise. While the reason for such a discrepancy is still not clear, a lack of IFN-γ expression in our disease model could not be incriminated. Indeed, in agreement with a previous report (33), we were able to detect a rise in IFN-γ following MPTP-induced nigrostriatal pathway injury. Whether different treatment protocols lead to distinct involvement of IFN-γ in disease models will need further clarification.

The requirement of FasL in CD4$^+$ T cell–mediated cytotoxicity is consistent with the finding that Fas-deficient mice display attenuated MPTP-induced DN loss (34), although another study has come to a different conclusion (35). Whereas, in the context of antigen presentation, the Fas/FasL pathway has been implicated in the deletion of activated macrophages, thereby contributing to the resolution of inflammation (36), recent evidence suggests that this pathway may instead induce proinflammatory cytokine responses in tissue macrophages (37). CD4$^+$ Th FasL-mediated activation of microglial cells could therefore participate in the inflammatory reaction and DN degeneration. T cell–derived FasL may also mediate inflammatory responses in astrocytes, which are known to be particularly resistant to Fas-mediated cell death and express proinflammatory cytokines and chemokines upon Fas ligation (38). In line with this, Fas expression has been shown to be upregulated on these glial cells both in PD patients and in the MPTP model (34, 39). Alternatively, infiltrated CD4$^+$ T cells may also induce DN cell demise through cell-cell contact. Such a mechanism has previously been shown in vitro, in which antigen primed CD4$^+$ or CD8$^+$ T cells induced neuronal death independently of antigen presentation and involved cell surface expression of FasL by activated T cells (40). Further investigations will be required to determine whether or not CD4$^+$ T cell–mediated cytotoxicity relies strictly on MHC-dependent antigen presentation.

In our disease model, the finding that harmful lymphocyte response is CD4 T cell–dependent but IFN-γ–independent raises important but still unresolved concerns about the phenotypic characteristics of these CD4 T cells. Although these observations would not favor the contribution of a Th1-type response, one can not exclude the possibility that CD4$^+$ Th1 cells may mediate cytotoxicity independently of IFN-γ as previously reported (40, 41). In particular, the role of other proinflammatory Th cytokines, such as TNF-α in T cell–mediated DN cell death, should also be considered as a potential deleterious mechanism, even though the role of this factor is still debated (42–44). Finally, another tantalizing possibility could be the involvement of an alternative inflammatory CD4 T cell population, namely, the recently described, Th17 cells. A growing body of evidence indicates that Th17 cells play a critical function not only in protection against microbial challenges but also in many organ-specific autoimmune diseases, including multiple sclerosis and its disease model experimental autoimmune encephalomyelitis (45). In line with this, it has recently been shown that Th17 cells have the potential of killing neurons, probably through the granzyme B cytolytic enzyme system (46). Whether such a CD4 T cell subset is implicated in parkinsonism as well merits further considerations.

It is worth noting that the CD4$^+$ T cell response to neurodegenerative processes can differently affect disease outcome. Indeed, while in the MPTP mouse model of PD, CD4$^+$ T cells are likely harmful to DNs (Figure 4A and ref. 32), it has recently been documented that this T cell population can provide supportive neuroprotection in animal model of inherited amyotrophic lateral sclerosis (ALS), by stimulating the trophic properties of glia (47). Interestingly, such pathological improvement can be recapitulated by delivering activated regulatory or effector T cells to ALS mice but not by Copolimer-1 immunization, indicating that antigen-driving Th2/Th3 responses are impaired in this animal model (48). Thus, different neurodegenerative contexts could result in distinct T cell responses, which in turn may positively or negatively influence disease progression. Undoubtedly, a better phenotypic characterization of these CD4$^+$ T cell subsets should improve our understanding of the role of the adaptive immune system in various neurodegenerative conditions.

In summary, we have shown that peripheral T cells infiltrate the brain parenchyma at the site of neuronal injury both in PD patients and in experimental parkinsonism. We have demonstrated that this cell-mediated immune response contributes to DN cell degeneration through a CD4$^+$ T cell–dependent Fas/FasL cytotoxic pathway. Our results, together with recent investigations (32), provide further rationale for targeting the adaptive arm of the immune system in PD. Therapeutic strategies may involve developing vaccines for antigens that promote cell-mediated antiinflammatory responses (49, 50) as well as blocking the migration of immune

cells across the BBB (51). Besides providing potential neuroprotective benefits for the remaining DNs, these immunomodulatory strategies may also be of interest for cell transplantation therapies, as long-term survival of grafted DNs, which eventually undergo PD-related pathological changes over time, could be jeopardized by such an immune-related hostile microenvironment (52).

Methods

Human samples. The study was performed on autopsy brainstem tissue (Hôpital de la Salpêtrière) from 8 control subjects and 14 parkinsonian patients, which were well-characterized clinically and neuropathologically. PD patients and control subjects did not differ significantly in terms of their mean age at death (PD patients, 77.85 ± 2.11 years of age; controls, 76.62 ± 3.72 years of age; $P = 0.76$, Student's *t* test; mean ± SEM) or the mean interval from death to the freezing of tissue (PD patients, 40.55 ± 3.80 hours; controls, 28.10 ± 7.08 hours; $P = 0.11$, Student's *t* test; mean ± SEM). Experiments using human postmortem material were approved by the Comité de Protection des Personnes review board (Ile de France 1, Paris, France). Due to limited accessibility to tissue sections, different numbers of patients were analyzed with respect to each leukocyte marker. Tissue was fixed in formaldehyde and then embedded in paraffin. Paraffin-embedded tissues were cut in serial 8-μm thick slices on a microtome, and sections were recovered on SuperFrost Plus slides (Kindler O GmbH), before incubation at 56°C for 3 days. Human tonsil slices (Dako) were used as tissue control for lymphoid marker immunohistochemistry.

Animals. Ten- to twelve-week-old male C57BL/6J mice, weighing 25–30 g (CERJ) were used. The following strains were obtained from The Jackson Laboratory: B6.129S6-*Cd4*^{tm1Knw}/J, B6.129S2-*Cd8a*^{tm1Mak}/J, B6.129P2-*Tcrb*^{tm1Mom}/J, B6.129S7-*Rag1*^{tm1Mom}/J, B6.129S7-*Ifng*^{tm1Ts}/J, B6Smn.C3-Faslgld/J, and corresponding parental WT inbred C57BL/6J. Mice were kept in a temperature-controlled room (23°C ± 1°C) under a 12-hour light/dark cycle and had ad libitum access to food and water. All animals were further genotyped after their sacrifice according to The Jackson Laboratory protocols. GFP$^+$ cells were isolated from double Tie2-Cre$^+$/ZEG$^+$ transgenic mice (designated GFP-Tg), in which the GFP reporter gene is expressed in early hematopoietic cell precursors (53). Animal handling was carried out according to ethical regulations and guidelines (*Guide for the care and use of laboratory animals*. NIH publication no. 85-23. Revised 1985) and the European Communities Council Directive 86/609/EEC. Experiments using vertebrates were approved by the Services Vétérinaires de Paris.

Treatment and tissue preparation. Groups of mice received 4 i.p. injections of MPTP-HCl (20 mg/kg, except where otherwise stated) at 2-hour intervals and were sacrificed from 6 hours to 21 days after the last injection. Control mice received saline solution only. For immunohistochemistry, mice were euthanized with 100 mg/kg pentobarbital and transcardially perfused first with 50 ml of heparin solution (5 U/ml) and then with 100 ml of 4% paraformaldehyde. Brain and spleen free-floating sections were prepared as described elsewhere (54). For HPLC analysis of MPP$^+$ levels, brains were rapidly removed from the skull and striata were dissected on humidified filters at 4°C. Tissues were then immersed in appropriate buffer.

Passive transfers. Single-cell suspensions were prepared from spleen and/or lymph nodes isolated from Tie2-Cre$^+$/ZEG$^+$, *gld*, *Ifng*$^{-/-}$, or C57BL/6J mice. GFP$^+$ T and B cells were purified with a cell magnetic separator (MACS, Miltenyi Biotech) according to the manufacturer's procedure, using anti-TCRβ (H57-597), anti-CD3ε (145-2C11), anti-CD4 (H-129.19), anti-CD8α (53-6.7), and anti-B220 PE-conjugated antibodies (all from BD Biosciences — Pharmingen) and anti–PE-conjugated MicroBeads (Miltenyi Biotech). Cells labeled with MicroBeads were retained on the MACS Column while unlabeled cells passed through. The column was removed from the separator, and the retained cells were eluted as the enriched, positively selected cell fraction. The enrichment of cells was confirmed by flow cytometry analysis using a FACSCalibur (Becton Dickinson) (e.g., more than 95% for T cells; Supplemental Figure 2A). Recipient *Rag1*$^{-/-}$ mice received a single i.v. injection of either 10^7 GFP$^+$ T cells or 2.5 10^7 GFP$^+$ B cells or 2 injections, 4 hours apart, of 10^7 total splenocytes (either *gld*, *Ifng*$^{-/-}$, or WT) in 0.2 ml phosphate buffered saline solution. Reconstitutions of GFP-expressing T and B lymphocytes in *Rag1*$^{-/-}$ recipient mice were checked by FACS analysis of blood samples collected from reconstituted *Rag1*$^{-/-}$ recipient mice prior to MPTP treatment or from lymph nodes after the mice were sacrificed (Supplemental Figure 2C). Three to four weeks after transfer, mice were intoxicated with MPTP or received an equal volume of saline solution.

Immunohistochemistry. Human sections were first deparaffinized in 2 changes of xylene for 5 minutes each. They were hydrated in 2 changes of 100%, 95%, then 75% ethanol and rinsed in distilled water. Antigen demasking was performed at 90°C–95°C for 30 minutes in citrate buffer, pH 6, (for CD8, CD20, CD79a, and CD57 staining) or EDTA buffer, pH 8, for CD4 staining. Sections were then allowed to cool down for 20 minutes before being rinsed in 0.25 M Tris buffer.

Human sections were pretreated with 0.01% H_2O_2/20% methanol, followed by 0.5% Triton and by normal goat serum (1:30; 30 minutes). They were then incubated at 4°C for 48 hours with anti-CD8 (1:50; Dako), anti-CD4 (1:20; Novocastra), anti-CD79α (1:100; Novocastra), anti-CD20 (1:100; L26, Novocastra), or anti-CD57 (1:50; Zymed).

Immunohistochemical staining on mouse brain sections was performed as previously described (51). The following primary antibodies were used: anti-TH (1:1,000; Peel Freez Biochemicals), anti–Mac-1/CD11b (1:250; Serotec), anti-GFAP (astrocytes, 1:5,000; Dako), anti-GFP (1:1,000; Invitrogen), anti-CD3 (1:1,000; Serotec), anti-CD8 (1:100; Serotec), or anti-CD4 (1:100; Serotec). Staining was revealed by the ABC method (Vector Laboratories) with 3,3′-diaminobenzidine (DAB) as the peroxidase substrate. Mouse sections were counterstained with thionin solution (Nissl stain), whereas human sections were counterstained with H&E solution.

For double-staining experiments, brain sections were simultaneously incubated with 2 primary antibodies developed in different species: anti-TH (1:1,000; Peel Freez Biochemicals), anti-GFP (1:1,000; Invitrogen), anti–Glut-1 (1:300; Santa Cruz Biotechnology Inc.), anti-PCNA (1:500; Dako), anti–Mac-1 (1:250; Serotec), anti-GFAP (1:5000; Dako), anti-CD3 (1:1,000; Serotec), anti-CD8 (1:100; Serotec), anti-CD4 (1:100; Serotec), anti–ICAM-1 (1:50; Serotec), anti-albumin (1:1,000; Cappel, MP Biomedicals), and anti-p17 caspase-3 (R&D Systems). Sections were then incubated in specific CY3- or FITC-conjugated secondary antibodies (Jackson ImmunoResearch Laboratories Inc.) at 1:250 dilution for 90 minutes at room temperature. For PCNA staining, sections were pretreated in 30% ethanol for 2 minutes and 70% ethanol at –20°C for 20 minutes. Hoechst nuclear staining was performed as previously described (53).

Electron microscopy. Ultrastructural analysis of T cells in the SNpc was performed as previously described with minor modifications (55). In brief, small blocks of mesencephalon containing the SNpc were fixed in a mixture of 4% paraformaldehyde and 2.5% glutaraldehyde. Sections 50-μm thick were cut and labeled for CD8 as described above. Following identification of CD8$^+$ cells, small areas of the sections were then excised and post-fixed in 1% osmium tetroxide for 30 minutes, rinsed in distilled water, dehydrated in a graded series of ethanol solutions, and embedded in Epon. Ultrathin (70 nm) sections were cut, counterstained with conventional techniques, and analyzed with a JEOL 1200EX II electron microscope at 80 kV.

Measurement of striatal dopamine. Striatal levels of dopamine and its metabolites (DOPAC, HVA) were determined by HPLC as previously reported (42).

Measurement of striatal MPP$^+$. Mice were killed 90 minutes after 1 i.p. injection of 30 mg/kg MPTP-HCl, and their striata were recovered and processed for HPLC, using UV detection (295-nm wavelength) to measure MPP$^+$ as described elsewhere (56).

Antibody array. C57BL/6J mice (n = 5 per group) were intoxicated with MPTP and sacrificed from 12 hours to 7 days after the last injection. Controls received an equal volume of saline solution. The expression level of various cytokines in protein homogenates prepared from the ventral mesencephalon was analyzed using a mouse antibody array glass chip (RayBio Mouse Cytokine Antibody Array G series 1000, RayBiotech Inc.). Incubation and washes were done according to the manufacturer's instructions. Briefly, chip arrays were blocked at room temperature for 30 minutes before being incubated with 50–100 μl of each sample at room temperature for 2 hours. Glass chips were then washed and incubated with biotin-conjugated primary antibody and Alexa Fluor 555–conjugated streptavidin according to the manufacturer's instructions. Fluorescence detection and analysis were performed using an Axon GenePix laser scanner.

Image and data analysis. DAB-immunostained sections were analyzed by bright-field microscopy, using a Leitz microscope equipped with image analysis software (Mercator, ExploraNova). TH^+ and $Nissl^+$ cell bodies were quantified stereologically on regularly spaced sections covering the whole SNpc using the VisioScan stereology tool. The investigator performing the quantification was blinded to the treatment and genotype groups during the analysis. Fluorescent sections were analyzed on a Zeiss Axioplan 2 using ExploraNova FluoUp 1.0 software.

Statistics. All values are expressed as the mean ± SEM. Differences in means between 2 groups were analyzed using 2-tailed Student's t test or, when data were not normally distributed, with a nonparametric Mann-Whitney U test. Differences in means among multiple data sets were analyzed using 1- or 2-way ANOVA with time, treatment, or genotype as the independent factors. When ANOVA showed significant differences, pair-wise comparisons between means were tested by Tukey post-hoc analysis. When data were not normally distributed, ANOVA on ranks was used (Kruskal-Wallis test followed by pairwise comparison using Dunn test). In all analyses, P values of less than 0.05 were considered significant (SigmaStat Statistical Software, Jandel Scientific).

Acknowledgments

We thank C. Combadière and C. Lobsiger for helpful discussions, V. Sazdovitch for assistance in collecting postmortem material, and T. Welte for providing $Tie2\text{-}Cre^+/ZEG^+$ double transgenic mice. This work was supported by grants from The Michael J. Fox Foundation (S. Hunot and E.C. Hirsch), Fondation pour la Recherche sur le Cerveau (S. Hunot), Fondation France Parkinson (V. Brochard), and the German Academic Exchange Service (D. Alvarez-Fischer). R.A. Flavell is an investigator at the Howard Hughes Medical Institute. E.C. Hirsch and S. Hunot are investigators at the Centre National de la Recherche Scientifique (CNRS).

Received for publication June 11, 2008, and accepted in revised form November 12, 2008.

Address correspondence to: Stéphane Hunot or Etienne C. Hirsch, INSERM UMR 679, Hôpital de la Salpêtrière, 47 Bd de l'Hôpital, 75013 Paris, France. Phone: 33-14-21-62-172; Fax: 33-14-42-43-658; E-mail: stephane.hunot@upmc.fr (S. Hunot). Phone: 33-14-21-62-202; Fax: 33-14-42-43-658; E-mail: etienne.hirsch@upmc.fr (E.C. Hirsch).

1. Dauer, W., and Przedborski, S. 2003. Parkinson's disease: mechanisms and models. *Neuron.* **39**:889–909.
2. Chen, H., et al. 2005. Nonsteroidal antiinflammatory drug use and the risk for Parkinson's disease. *Ann. Neurol.* **58**:963–967.
3. Wahner, A.D., Bronstein, J.M., Bordelon, Y.M., and Ritz, B. 2007. Nonsteroidal anti-inflammatory drugs may protect against Parkinson disease. *Neurology.* **69**:1836–1842.
4. Nagatsu, T., Mogi, M., Ichinose, H., and Togari, A. 2000. Changes in cytokines and neurotrophins in Parkinson's disease. *J. Neural Transm. Suppl.* **60**:277–290.
5. Czlonkowska, A., Kurkowska-Jastrzebska, I., Czlonkowski, A., Peter, D., and Stefano, G.B. 2002. Immune processes in the pathogenesis of Parkinson's disease — a potential role for microglia and nitric oxide. *Med. Sci. Monit.* **8**:RA165–RA177.
6. Whitton, P.S. 2007. Inflammation as a causative factor in the aetiology of Parkinson's disease. *Br. J. Pharmacol.* **150**:963–976.
7. McGeer, P.L., Itagaki, S., Akiyama, H., and McGeer, E.G. 1988. Rate of cell death in parkinsonism indicates active neuropathological process. *Ann. Neurol.* **24**:574–576.
8. Hunot, S., et al. 1999. FcεRII/CD23 is expressed in Parkinson's disease and induces, in vitro, production of nitric oxide and tumor necrosis factor-α in glial cells. *J. Neurosci.* **19**:3440–3447.
9. Kurkowska-Jastrzebska, I., et al. 1999. The inflammatory reaction following 1-methyl-4-phenyl-1,2,3,6-tetrahydropyridine intoxication in mouse. *Exp. Neurol.* **156**:50–61.
10. Janeway, C.A., Jr., and Travers, P. 1997. *Immunobiology: the immune system in health and disease*. 3rd edition. Garland Publishing Inc. New York, New York, USA. A1–A10.
11. Kortekaas, R., et al. 2005. Blood-brain barrier dysfunction in parkinsonian midbrain in vivo. *Ann. Neurol.* **57**:176–179.
12. Engelhardt, B. 2006. Molecular mechanisms involved in T cell migration across the blood-brain barrier. *J. Neural Transm.* **113**:477–485.
13. Serpe, C.J., Kohm, A.P., Huppenbauer, C.B., Sanders, V.M., and Jones, K.J. 1999. Exacerbation of facial motoneuron loss after facial nerve transection in severe combined immunodeficient (*scid*) mice. *J. Neurosci.* **19**:RC7.
14. Chen, Z., Ljunggren, H.G., Zhu, S.W., Winblad, B., and Zhu, J. 2004. Reduced susceptibility to kainic acid-induced excitotoxicity in T-cell deficient CD4/CD8 (–/–) and middle-aged C57BL/6 mice. *J. Neuroimmunol.* **146**:33–38.
15. Mombaerts, P., et al. 1992. Mutations in T-cell antigen receptor genes alpha and beta block thymocyte development at different stages. *Nature.* **360**:225–231.
16. Fung-Leung, W.P., et al. 1991. CD8 is needed for development of cytotoxic T-cells but not helper T-cells. *Cell.* **65**:443–449.
17. Rahemtulla, A., et al. 1991. Normal development and function of CD8+ cells but markedly decreased helper cell activity in mice lacking CD4. *Nature.* **353**:180–184.
18. Mount, M.P., et al. 2007. Involvement of interferon-γ in microglial-mediated loss of dopaminergic neurons. *J. Neurosci.* **27**:3328–3337.
19. Takahashi, T., et al. 1994. Generalized lymphoproliferative disease in mice, caused by a point mutation in the Fas ligand. *Cell.* **76**:969–976.
20. Hunot, S., and Hirsch, E.C. 2003. Neuroinflammatory processes in Parkinson's disease. *Ann. Neurol.* **53**(Suppl. 3):S49–S60.
21. Baba, Y., Kuroiwa, A., Uitti, R.G., Wszolek, Z.K., and Yamada, T. 2005. Alterations of T-lymphocyte populations in Parkinson disease. *Parkinsonism Relat. Disord.* **11**:493–498.
22. Cose, S., Brammer, C., Khanna, K.M., Masopust, D., and Lefrançois, L. 2006. Evidence that a significant number of naive T cells enter non-lymphoid organs as part of a normal migratory pathway. *Eur. J. Immunol.* **36**:1423–1433.
23. Togo, T., et al. 2002. Occurrence of T cells in the brain of Alzheimer's disease and other neurological diseases. *J. Neuroimmunol.* **124**:83–92.
24. German, D.C., et al. 1996. The neurotoxin MPTP causes degeneration of specific nucleus A8, A9 and A10 dopaminergic neurons in the mouse. *Neurodegeneration.* **5**:299–312.
25. Farkas, E., De Jong, G.I., de Vos, R.A., Jansen Steur, E.N., and Luiten, P.G. 2000. Pathological features of cerebral cortical capillaries are double in Alzheimer's disease and Parkinson's disease. *Acta Neuropathol.* **100**:395–402.
26. Haussermann, P., Kuhn, W., Przuntek, H., and Muller, T. 2001. Integrity of the blood-cerebrospinal fluid barrier in early Parkinson's disease. *Neurosci. Lett.* **300**:182–184.
27. Adams, J.D., Jr., Klaidman, L.K., Odunze, I.N., and Johannenssen, J.N. 1991. Effects of MPTP on the cerebrovasculature. *Int. J. Dev. Neurosci.* **9**:155–159.
28. Zhao, C., Ling, Z., Newman, M.B., Bhatia, A., and Carvey, P.M. 2007. TNF-α knockout and minocycline treatment attenuates blood-brain barrier leakage in MPTP-treated mice. *Neurobiol. Dis.* **26**:36–46.
29. Springer, T.A. 1994. Traffic signals for lymphocyte recirculation and leukocyte emigration: the multistep paradigm. *Cell.* **76**:301–314.
30. Miklossy, J., et al. 2005. Role of ICAM-1 in persisting inflammation in Parkinson disease and MPTP monkeys. *Exp. Neurol.* **197**:275–283.
31. Jenner, P., and Olanow, C.W. 1998. Understanding cell death in Parkinson's disease. *Ann. Neurol.* **44**(Suppl. 1):S72–S84.
32. Benner, E.J., et al. 2008. Nitrated α-synuclein immunity accelerates degeneration of nigral dopaminergic neurons. *PloS ONE.* **3**:e1376.
33. Ciesielska, A., et al. 2003. Dynamics of expression of the mRNA for cytokines and inducible nitric synthase in a murine model of the Parkinson's disease. *Acta Neurobiol. Exp. (Wars.)* **63**:117–126.
34. Hayley, S., et al. 2004. Regulation of dopaminergic loss by Fas in a 1-methyl-4-phenyl-1,2,3,6-tetrahydropyridine model of Parkinson's disease. *J. Neurosci.* **24**:2045–2053.
35. Landau, A.M., et al. 2005. Defective Fas expression

exacerbates neurotoxicity in a model of Parkinson's disease. *J. Exp. Med.* **202**:575–581.
36. Ashany, D., et al. 1995. Th1 CD4+ lymphocytes delete activated macrophages through the Fas/APO-1 antigen pathway. *Proc. Natl. Acad. Sci. U. S. A.* **92**:11225–11229.
37. Park, D.R., et al. 2003. Fas (CD95) induces proinflammatory cytokine responses by human monocytes and monocyte-derived macrophages. *J. Immunol.* **170**:6209–6216.
38. Choi, C., and Benveniste, E.N. 2004. Fas ligand/fas system in the brain: regulator of immune and apoptosis responses. *Brain Res. Rev.* **44**:65–81.
39. Ferrer, I., Blanco, R., Cutillas, B., and Ambrosio, S. 2000. Fas and Fas-L expression in Huntington's disease and Parkinson's disease. *Neuropathol. Appl. Neurobiol.* **26**:424–433.
40. Giuliani, F., Goodyer, C.G., Antel, J.P., and Yong, V.W. 2003. Vulnerability of human neurons to T cell-mediated cytotoxicity. *J. Immunol.* **171**:368–379.
41. Ju, S.T., Cui, H., Panka, D.J., Ettinger, R., and Marshak-Rothstein, A. 1994. Participation of target Fas protein in apoptosis pathway induced by CD4+ Th1 and CD8+ cytotoxic T cells. *Proc. Natl. Acad. Sci. U. S. A.* **91**:4185–4189.
42. Rousselet, E., et al. 2002. Role of TNF-alpha receptors in mice intoxicated with the parkinsonian toxin MPTP. *Exp. Neurol.* **177**:183–192.
43. Ferger, B., Leng, A., Mura, A., Hengerer, B., and Feldon, J. 2004. Genetic ablation of tumor necrosis factor–alpha (TNF-alpha) and pharmacological inhibition of TNF-synthesis attenuates MPTP toxicity in mouse striatum. *J. Neurochem.* **89**:822–833.
44. Sriram, K., Miller, D.B., and O'Callaghan, J.P. 2006. Minocycline attenuates microglial activation but fails to mitigate striatal dopaminergic neurotoxicity: role of tumor necrosis factor-alpha. *J. Neurochem.* **96**:706–718.
45. Zhu, J., and Paul, W.E. 2008. CD4 T cells: fates, functions, and faults. *Blood.* **112**:1557–1568.
46. Kebir, H., et al. 2007. Human Th17 lymphocytes promote blood-brain barrier disruption and central nervous system inflammation. *Nat. Med.* **13**:1173–1175.
47. Beers, D.R., Henkel, J.S., Zhao, W., Wang, J., and Appel, S.H. 2008. CD4+ T cells support glial neuroprotection, slow disease progression, and modify glial morphology in an animal model of inherited ALS. *Proc. Natl. Acad. Sci. U. S. A.* **105**:15558–15563.
48. Banerjee, R., et al. 2008. Adaptive immune neuroprotection in G93A-SOD1 amyotrophic lateral sclerosis mice. *PLoS ONE.* **3**:e2740.
49. Benner, E.J., et al. 2004. Therapeutic immunization protects dopaminergic neurons in a mouse model of Parkinson's disease. *Proc. Natl. Acad. Sci. U. S. A.* **101**:9435–9440.
50. Reynolds, A.D., et al. 2007. Neuroprotective activities of CD4+CD25+ regulatory T cells in an animal model of Parkinson's disease. *J. Leukoc. Biol.* **82**:1083–1094.
51. Luster, A.D., Alon, R., and von Andrian, U.H. 2005. Immune cell migration in inflammation: present and future therapeutic targets. *Nat. Immunol.* **6**:1182–1190.
52. Braak, H., and Del Tredici, K. 2008. Assessing fetal nerve cell grafts in Parkinson's disease. *Nat. Med.* **14**:483–485.
53. Welte, T., et al. 2003. STAT3 deletion during hematopoiesis causes Crohn's disease-like pathogenesis and lethality: A critical role of STAT3 in innate immunity. *Proc. Natl. Acad. Sci. U. S. A.* **100**:1879–1884.
54. Hunot, S., et al. 2004. JNK-mediated induction of cyclooxygenase 2 is required for neurodegeneration in a mouse model of Parkinson's disease. *Proc. Natl. Acad. Sci. U. S. A.* **101**:665–670.
55. Hunot, S., et al. 1997. Nuclear translocation of NF-kappaB is increased in dopaminergic neurons of patients with Parkinson disease. *Proc. Natl. Acad. Sci. U. S. A.* **94**:7531–7536.
56. Liberatore, G.T., et al. 1999. Inducible nitric oxide synthase stimulates dopaminergic neurodegeneration in the MPTP model of Parkinson disease. *Nat. Med.* **5**:1403–1409.